# *Basket Modification Concepts for Disposal Reactivity Control of Dual Purpose Canisters*

## Spent Fuel and Waste Disposition

*Prepared for*
*US Department of Energy*
*Spent Fuel and Waste Science and Technology*

*Justin Clarity, Kaushik Banerjee, and Paul Miller*
*Oak Ridge National Laboratory*

*January 29, 2021*

**M3SF-21OR010305125**
**ORNL/SPR-2021/1780**

**SFWD Working Document: External Release or Reference Requires DOE-NE Approval**

# SUMMARY

This report documents work performed supporting the US Department of Energy (DOE) Office of Nuclear Energy (NE) Spent Fuel and Waste Disposition (SFWD), Spent Fuel and Waste Science and Technology, under work breakdown structure element 1.08.01.03.05, "Direct Disposal of Dual Purpose Canisters." In particular, this report fulfills milestone M3SF-21OR010305125, "DPC criticality analysis with fuel/basket modification," within work package SF-21OR01030512, "DPC Reactivity and Criticality Modeling—ORNL."

This report uses three of the most reactive canisters that have been analyzed to-date using UNF-ST&DARDS to examine the performance of three potential reactivity suppression technologies under disposal conditions. Three already loaded canisters were analyzed using as-loaded contents including TSC-37 and MPC-32 pressurized water reactor (PWR) dual-purpose canisters (DPCs) and the MPC-89 DPCs. The reactivity suppression technologies considered were the $B_4C$-filled disposal control rod assembly (DCRA) and the advanced neutron absorber (ANA)–based chevron insert for the PWR canisters and the ANA-based fuel channel replacement absorber for the MPC-89. For each combination of absorber concept and DPC, various insert patterns and absorber material concentrations were considered. The results of the analysis show that the DCRA concept has promise for providing reactivity hold-down for PWR DPCs, and the ANA fuel channel replacement absorber has promise for providing reactivity hold-down in BWR DPCs. The ANA chevron basket insert showed mixed results, providing sufficient reactivity hold-down in the lower reactivity canister, but failing to do so in the higher reactivity canister considered herein.

# ACKNOWLEDGMENTS

This research was sponsored by the Spent Fuel and Waste Science and Technology Program of the US Department of Energy and was carried out at Oak Ridge National Laboratory under contract DE-AC05-00OR22725 with UT-Battelle, LLC.

# CONTENTS

# LIST OF FIGURES

# REVISION HISTORY

| Revision | Changes Made |
|---|---|
| 0 | Initial issue |

# ACRONYMS

| | |
|---|---|
| ANA | advanced neutron absorber |
| BWR | boiling water reactor |
| DB | degraded basket |
| DCRA | disposal control rod assembly |
| DOE | US Department of Energy |
| DPC | dual-purpose canister |
| FEPs | features, events, and processes |
| NA | no absorber (loss of neutron absorber case) |
| NE | Office of Nuclear Energy |
| ORNL | Oak Ridge National Laboratory |
| PWR | pressurized water reactor |
| SFWD | Spent Fuel and Waste Disposition |
| UNF-ST&DARDS | Used Nuclear Fuel Storage, Transportation and Disposal Analysis Resource and Data System |

# BASKET MODIFICATION CONCEPTS FOR DISPOSAL REACTIVITY CONTROL OF DUAL PURPOSE CANISTERS

## 1. INTRODUCTION

The current spent nuclear fuel management strategy includes reliance on dry storage. Utilities are meeting their interim storage needs on an individual basis with the use of large-capacity dry storage casks. The focus is currently on meeting existing storage and transportation requirements, as disposal requirements are not currently available. The casks are commonly known as *dual-purpose canisters* (DPCs), serving the dual purposes of storage and transportation. However, a small percentage of single-purpose (storage only) systems is also being used to meet storage needs. This report investigates the post-closure criticality safety aspects of DPCs.

Placement of large, heavy waste packages containing DPCs into a repository for direct disposal has not yet been implemented domestically or internationally. Therefore, the prospect of direct disposal of DPCs presents new engineering and scientific challenges. Some of these challenges that have already been investigated, including handling and placement, use of ramps vs. shafts, use of hoists, use of transport equipment, and thermal management. Additionally, some studies were conducted to determine the feasibility of direct disposal from a criticality analysis perspective and concluded that, while direct disposal is possible, demonstrating subcriticality over the disposal time period is a challenge [1,2]. The alternative to directly disposing of DPCs in a repository is to repackage the spent nuclear fuel into smaller canisters for disposal. Direct disposal of DPCs without cutting them open and repackaging is appealing because it could be more cost effective, could reduce the complexity of fuel management operations both in and outside reactor facilities, and could result in lower cumulative worker doses during interim storage and handling before eventual disposal in a deep geologic repository.

The performance of the basket neutron absorber material as a function of time inside the canister is a key factor for demonstrating subcriticality. The neutron absorber panel material used in the majority of currently loaded DPCs is Boral®. Boral is composed of $B_4C$ particles and alloy 1100 aluminum that are hot-rolled together to form a neutron-absorbing core. The neutron-absorbing core is then bonded to two outer layers of alloy 1100 aluminum. Various corrosion tests have been performed on this material because it is used in existing casks and in spent fuel pools. Corrosion tests that were conducted under pool chemistry conditions showed that cladding material was lost at a rate of 0.28 mil per year, which equates to a service life of approximately 40 years (in the presence of water) before degradation of the neutron-absorbing core [1]. Additionally, some tests of Boral under simulated vacuum drying processes have shown the formation of blisters within the Boral induced by the drying process [3]. Considering that the repository periods of interest are expected to be at least 10,000 years, it is not likely that the Boral neutron absorber will maintain its criticality control function this long if the package cavity is exposed to an aqueous environment.

Within a repository performance assessment, features, events, processes (FEPs), and sequences of FEPs that might affect the repository, are examined. Criticality is considered such an event within the FEPs nomenclature with the potential to affect repository performance. Before a performance assessment is conducted, any FEPs that can affect repository performance are screened for inclusion or exclusion. Based on previous screening criteria, options available for excluding a feature, event, or process consisted of a low-probability criterion, a low-consequence criterion, and regulation. Previous work by Clarity et al. [4] showed that, in many cases, considering the as-loaded contents of DPCs is enough to offset the

potential degradation of the aluminum-based neutron absorbers. However, there are a substantial number of DPCs for which subcriticality cannot be demonstrated based on crediting the as-loaded contents alone.

The Used Nuclear Fuel Storage, Transportation and Disposal Analysis Resource and Data System (UNF-ST&DARDS) is a tool developed to perform analyses such as post-closure DPC reactivity estimation. This report extends the work reported in Clarity et al. [4] by incorporating various basket modification strategies in order to suppress reactivity. The basket modification analysis was performed by modifying the models of selected canisters that were analyzed in the prior work [4] to include proposed neutron absorbing technologies than can be credited in repository environments.

The remainder of this report is organized as follows: Section 2 discusses the canisters selected to perform the analysis, analyzes the contents of those canisters and outlines the types of materials and reactivity suppression strategies used in the remainder of the report; Section 3 presents the results of the various calculations and discusses the potential implications of those results; and Section 4 discusses the conclusions derived from this work.

# 2. METHODOLOGY

This section discusses the computational methods used, the canisters that were selected, the types of reactivity suppression devices considered, and the locations where the devices were placed within the canister in the cases analyzed.

## 2.1 Computational Methods

The burnup credit and criticality computational methods used to perform this work are discussed at length in Clarity et al. [4]. The same computational pipeline, ORIGEN reactor libraries, and DPC computational templates are used here as in the previous work [4]. All criticality calculations performed to support this work used the SCALE 6.2.3 version of the KENO-VI Monte Carlo code with ENDF/B-VII.1 nuclear data. The Monte Carlo parameters used herein are 550 generations of 50,000 neutron histories, skipping the first 50 generations to allow for source convergence. These parameters are sufficient to produce a Monte Carlo uncertainty on $k_{eff}$ of 0.00025 or less for all calculations. Because the Monte Carlo uncertainty is very small relative to the reactivity changes induced by the absorber materials, it is not included throughout the remainder of the document.

## 2.2 Selected Canisters

The three canisters selected to assess the reactivity suppression concepts were the highest reactivity canisters among the ~800 DPCs analyzed to-date and analysis times for the TSC-37, MPC-32, and MPC-89 designs.

**The TSC-37 canister model** selected for this work is the TSCDF-37-TSCDF-15 located at Zion and was evaluated in the year 22,000. This canister is loaded with Westinghouse 15 × 15 fuel assemblies. The TSC-37 has a basket with carbon steel structural components, so it is unclear what the performance of the basket will be over the repository performance assessment period. To account for the distinct possibilities that (1) either only the neutron absorber would degrade or (2) both the neutron absorber and the basket could degrade, calculations were performed for the loss of neutron absorber or no absorber (NA) and degraded basket (DB) conditions. The NA model is produced by replacing the NA material with water, and the DB case is produced by replacing both the neutron absorber material and basket material with water. The $k_{eff}$ for the NA case with no mitigating basket modification technology is 1.08619, and the $k_{eff}$ for the DB condition with no basket modification technology is 1.17033. To better understand the neutronic behavior of the TSC-37 canister selected for this work, a plot of the axial and radial fission densities is provided in Figure 1, and the individual assembly reactivities (k-infinity) are plotted in Figure 2. The fission densities in Figure 1 are tallied on a 2 cm cubic mesh during the criticality calculations, and

the assembly reactivities are calculated by running infinitely reflected (radially) criticality calculations for the individual assemblies with a pitch equal to the in-reactor pitch plus an additional 2 cm of water. The reactivity plots are colored so that assemblies with a $k_{inf}$ of 1.0 are white, and assemblies with a $k_{inf}$ 1.3 have the darkest shade of red, and the shades of red for all assemblies between 1.0 and 1.3 are darker or lighter, depending on the $k_{inf}$.

The fission density plot in Figure 1 indicates that the majority of the fissions are occurring in the upper three to four nodes of the nine center assemblies. This indicates that this area is the most important to focus on for reactivity suppression measures. The assembly reactivity values given in Figure 2 show that the most reactive assemblies in the canister are in the center nine assemblies and in the four assemblies loaded in the damaged fuel locations on the peripheries of the minor axes of the canister. The nine center assemblies were discharged from the last cycle of operation at Zion and include fuel that did not have the opportunity to be irradiated to the degree that a typical assembly would be as a result of plant shutdown. The nine center assemblies are also located in the lowest leakage locations in the canister. This loading pattern was likely chosen in order to optimize canister thermal performance, however, it results in a highly suboptimal loading from a criticality perspective. The four damaged fuel assemblies are modeled as fresh fuel of their actual enrichment, which is customary in this type of analysis, but they are also in the highest leakage locations in the canister.

**The MPC-32 model** selected for this work is the MPC-32-162 located at Farley and was evaluated in the year 22,000. The canister is loaded with Westinghouse 17 × 17 fuel assemblies. The MPC-32 canister is constructed with a stainless steel basket which is assumed to not degrade during the repository performance period, so only the NA case was modeled. The NA model was created by replacing the neutron absorber with water. The calculated $k_{eff}$ of the NA model is 1.02151. In order to better understand the neutronic behavior of the MPC-32 canister selected for this work a plot of the axial and radial fission densities is plotted in Figure 3 and the individual assembly reactivities are plotted in Figure 4. The same color scale is used for the assembly reactivities as was used above.

The fission density plots in Figure 3 show that the majority of the fissions are occurring in the upper two to three nodes of the center 16 assemblies, though there is significant skewing of the fission toward the lower portion of the radial plot of that 16 assembly region. The individual assembly reactivities in Figure 4 show that the MPC-32 is more homogenously loaded than is the case for the TSC-37 case, there are however, two assemblies which are more reactive than the others that are loaded toward the bottom of the middle 16 assembly region of the canister. Those two assemblies likely account for the skewing of the fission distribution.

**The MPC-89 model** selected for this work is the MPC-89-4803D-MPCFW021 canister located at Browns Ferry evaluated in the year 22,000. This represents the most reactive case of all of the MPC-89 cases. The canister is loaded with a variety of different BWR fuel assembly types. Calculations are performed only for the DB configuration for the MPC-89 canister because the basket is composed of a relatively new form of neutron absorber known as Metamic-HT®. Metamic-HT is a $B_4C$/aluminum mixture with a higher level of aluminum than a typical absorber panel. However, concerns similar to those for other neutron absorber materials remain. Since the loss of the neutron absorber would also represent a loss of the basket structure, the spacing between the assemblies was reduced to the inner dimension of the cell. The calculated $k_{eff}$ for the DB case is 1.18622. An axial and radial fission density plot for the MPC-89 canister is included in Figure 5, and the individual assembly reactivities are shown in Figure 6.

The fission density plot in Figure 5 indicates that there is a more or less even distribution of fissions across the top two to three nodes in the center three rings of the assemblies positioned around the center assembly. There also appears to be a slight depression of the fission distribution in the very center of the canister. Figure 6 indicates that the assembly reactivities are relatively homogenous, with the peripheral

assemblies having the lowest reactivity, and the assemblies in the center of the canister having slightly lower reactivity than the assemblies surrounding them. The lower reactivities in the center may cause the slight depression in the fission distribution in the center of the canister. It is noted that the canister reactivity is higher than the infinite medium assembly reactivities because there is a larger pitch in the assembly reactivity cases than in the DB model.

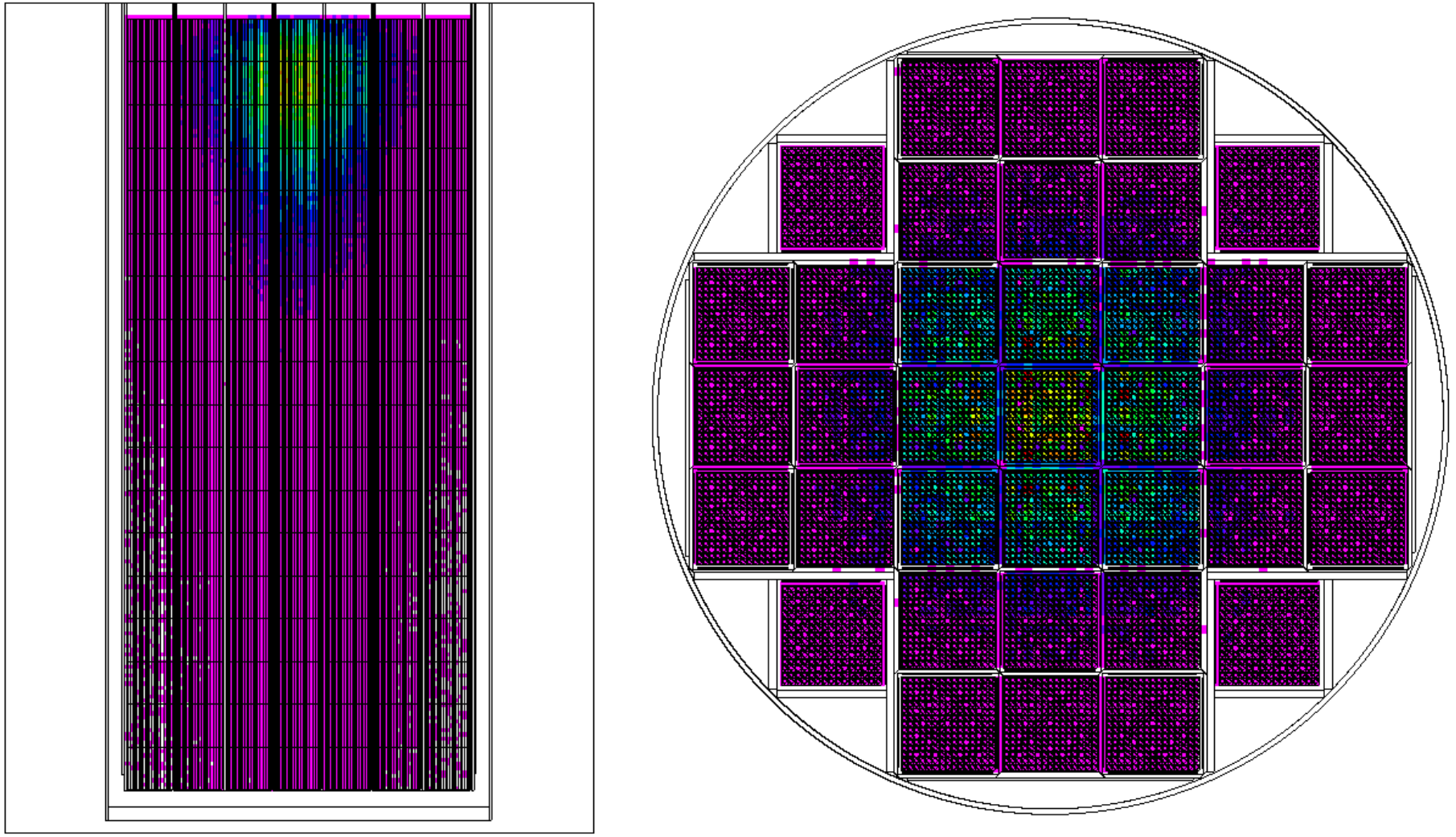

**Figure 1. Axial (left) and radial (right) fission density plots for the TSC-37 base case.**

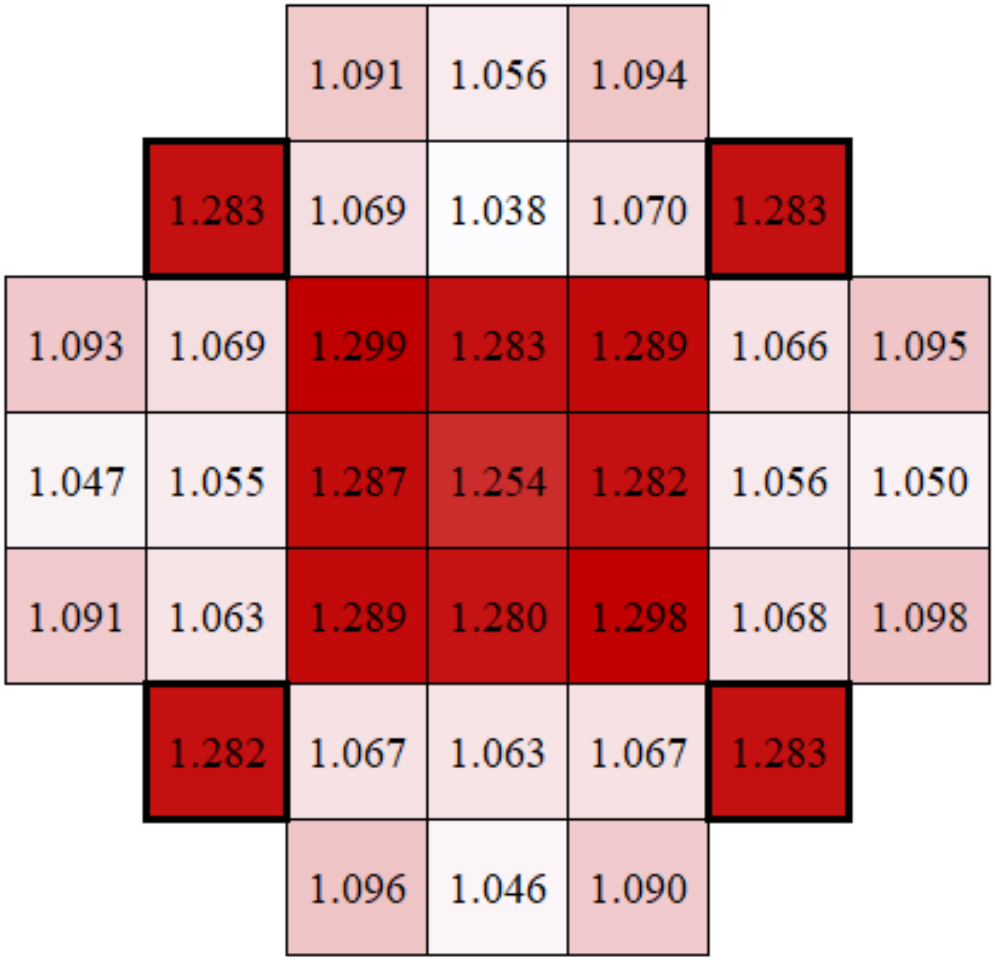


**Figure 2. Assembly reactivity ($k_{inf}$) by location for the TSC-37 canister.**

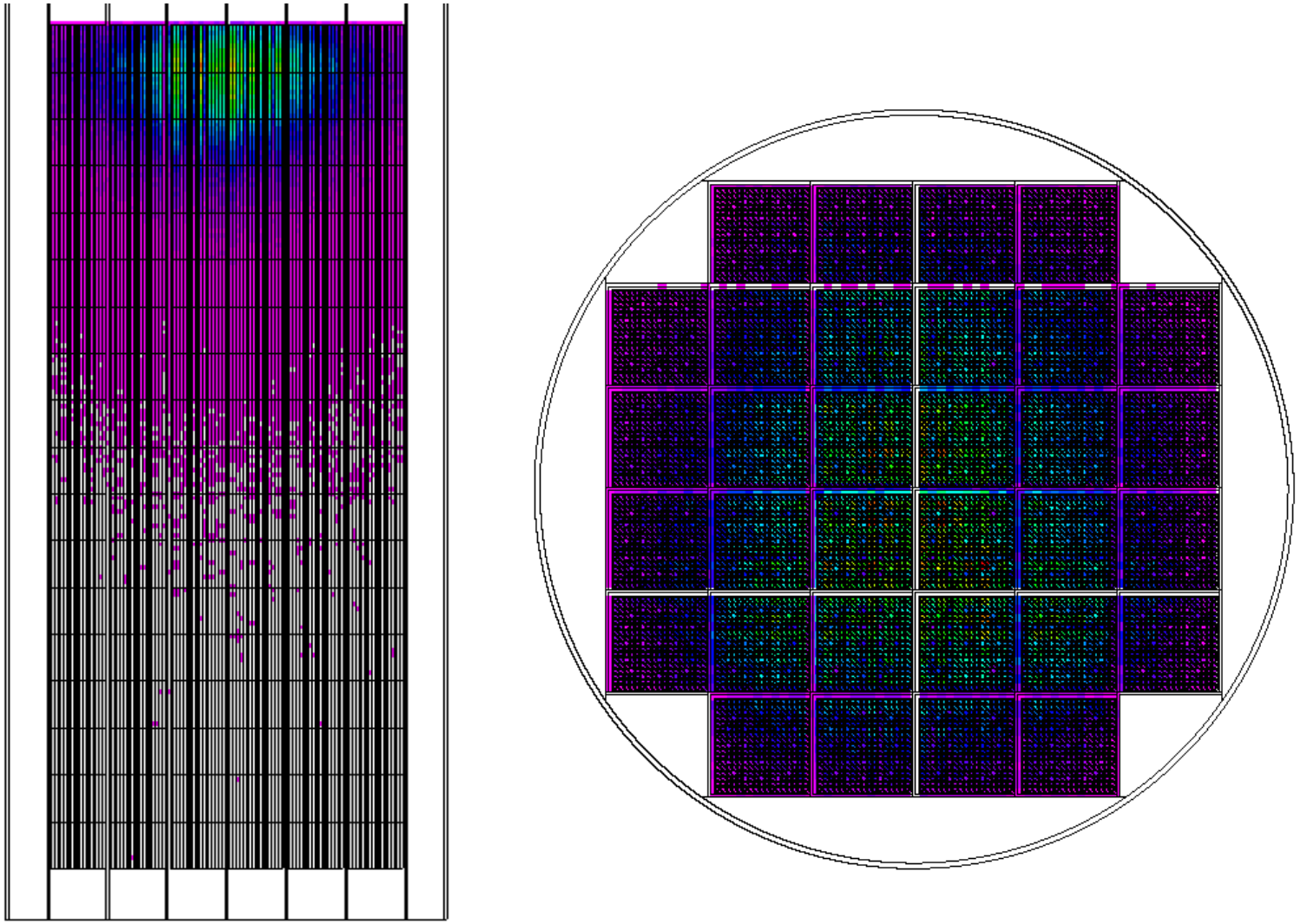

**Figure 3. Axial (left) and radial (right) fission density plots for the MPC-32 base case.**

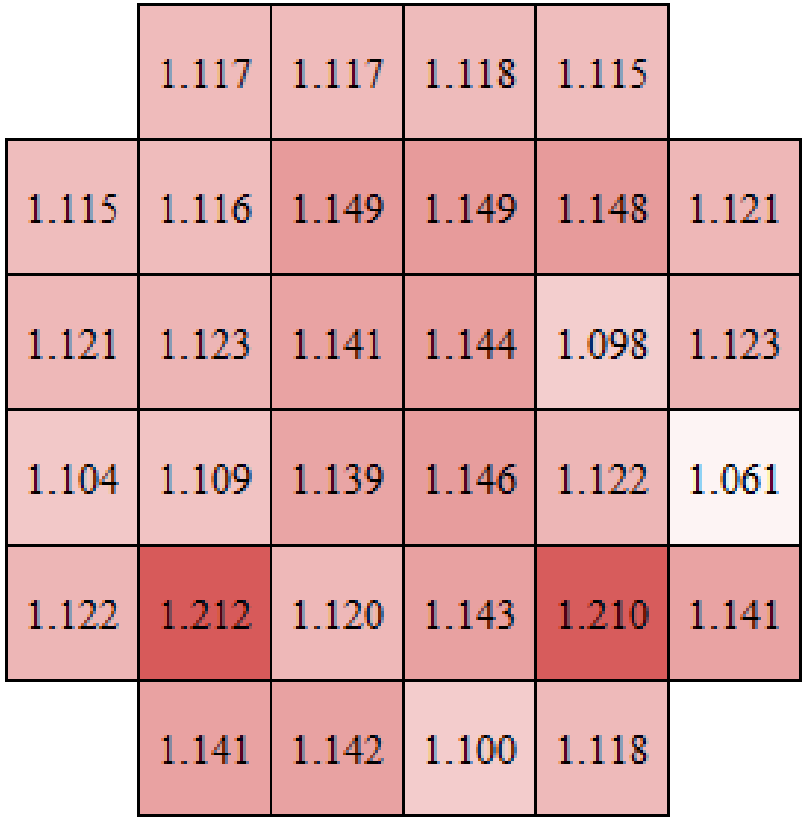


**Figure 4. Assembly reactivity ($k_{inf}$) by location for the MPC-32 canister.**

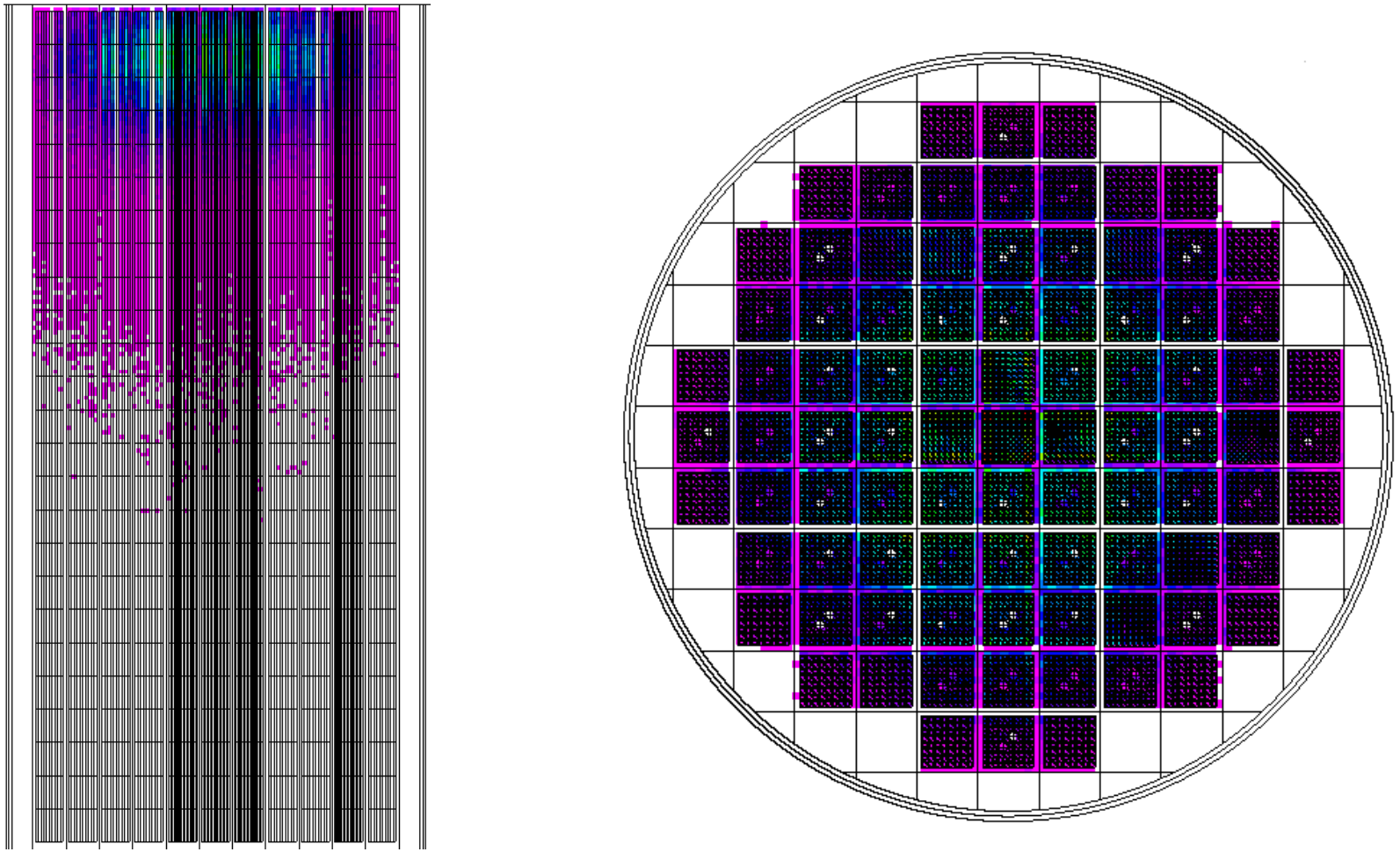

**Figure 5. Axial (left) and radial (right) fission density plots for the MPC-89 base case.**

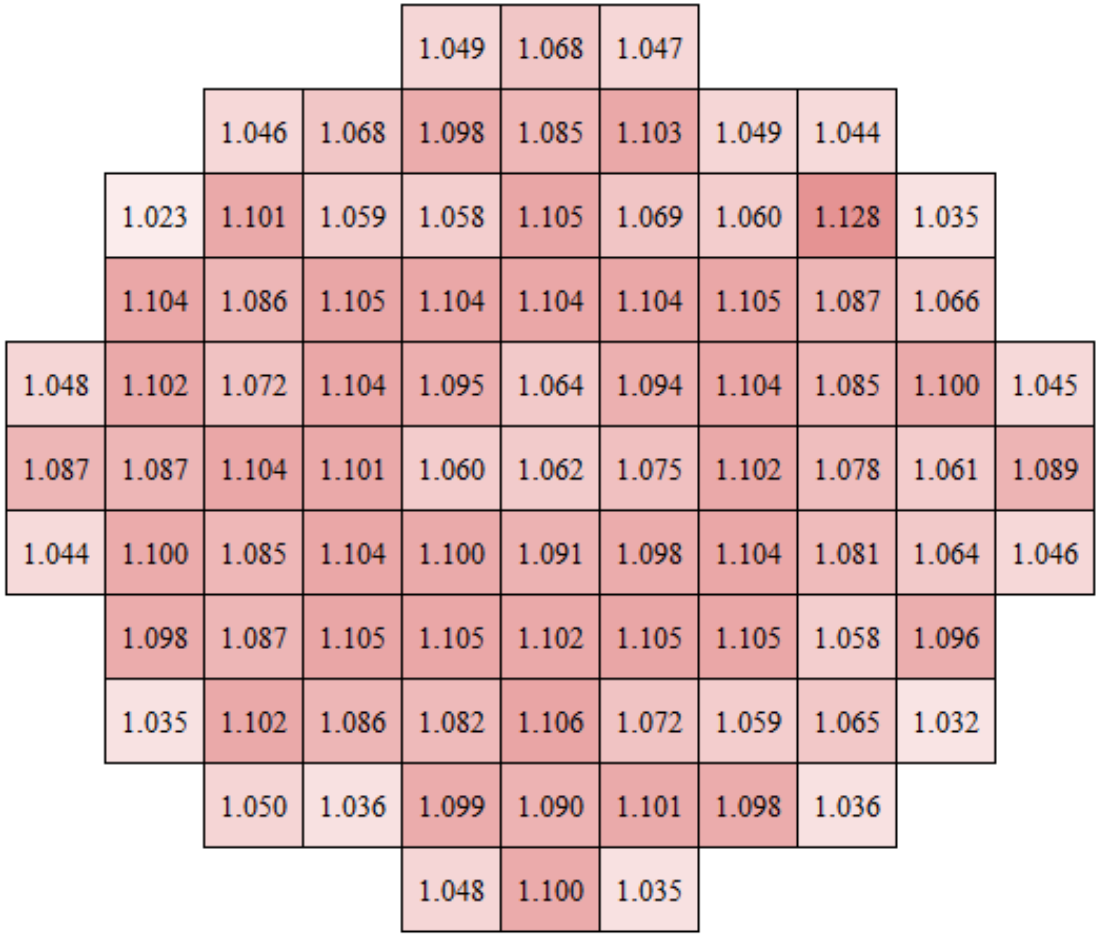


**Figure 6. Assembly reactivity ($k_{inf}$) by location for the MPC-89 canister.**

## 2.3 Absorber Types and Analyzed Configurations

Three absorber concepts are examined in this report based on the recommendations contained in *Options for Future Fuel/Basket Modifications for DPC Disposition* [5]. This section discusses the absorber concepts, their dimensions, the materials of construction, and their implementation in canister models to assess their feasibility.

The first concept proposed is the **disposal control rodlet assembly (DCRA)**. The DCRA is similar to a standard guide tube–based absorber, such as a control rod or burnable absorber that would typically be used for power distribution and excess reactivity control during normal PWR operation. The discussion provided in the work by Hardin and Donovan [5] indicates that natural $B_4C$ would be a likely material for this concept due to its low cost and high durability. To account for the possibility that it may not be possible or desirable to fabricate control materials from full-density $B_4C$, a range of weight fractions of $B_4C$ in the control materials was used, varying 0 to 100% $B_4C$. The dimensions for DCRA modeling used here were specified in Hardin and Donovan's report [5] for the DCRA and are as follows: (1) a pellet diameter of 8.4 mm, (2) a rodlet inner diameter of 8.88 mm, and (3) a rodlet outer diameter of 9.88 mm. The DCRA cladding material was conservatively modeled as void since the material is unknown at this time. This work analyzed two PWR DPCs, the first being a TSC-37 containing Westinghouse 15 × 15 fuel assemblies, and the second being an MPC-32 containing Westinghouse 17 × 17 fuel assemblies. The Westinghouse 15 × 15 fuel assembly has 20 guide tubes, and the Westinghouse 17 × 17 fuel assembly has 24 guide tubes. All guide tubes in each fuel assembly were modeled as containing DCRAs. A SCALE-generated depiction of a single basket cell from each model is shown in Figure 7, with the TSC-37 basket cell shown on the left, and the MPC-32 basket cell shown on the right, and with the fuel rods, DCRAs, and basket walls labeled. It is noted that the assemblies are off center in the MPC-32 model because this is consistent with the baseline model with the installed neutron absorbers present; when the absorbers are present, this space is needed to accommodate the assembly.

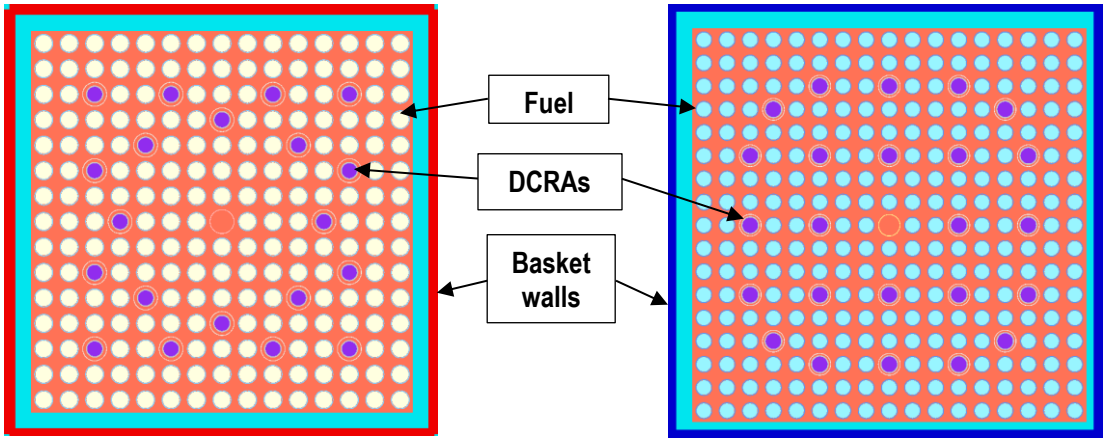


**Figure 7. SCALE-generated depiction of a Westinghouse 15 × 15 fuel assembly in a TSC-37 basket cell with 20 DCRAs (left) and a Westinghouse 17 × 17 fuel assembly in an MPC-32 basket cell with 24 DCRAs (right).**

The second concept is the chevron neutron absorber that would be mounted to the canister basket or the assembly top nozzles. The neutron absorber would need to be more durable in a repository environment than the typical aluminum-based absorber technology. The work by Hardin and Donovan [5] indicates that using the advanced neutron absorber (ANA) material currently under development may be appropriate for this purpose. The ANA materials discussed in Hardin and Donovan's report [5] are

described as Hastelloy-based alloys similar to Alloy C-4 or Alloy C-22, with natural gadolinium loaded into the material. For the purposes of this report, a composition for Alloy C-22 from Rolled Alloys [6] was used. The material was modeled as being 65.25 wt.% Ni, 13.5 wt.% Mo, and 21.25 wt.% Cr, with a density of 8.69 g/cm$^3$. These weight percentages represent midpoints of the specified values for the alloy's major constituents. The thickness of the specified insert from Hardin and Donovan [5] was 3 mm at manufacturing, but material degradation is expected to occur in the repository environment, so the ANA insert that was modeled was only 1 mm thick. The inserts were specified to be 20 cm wide for each of the two panels. Typically, some portion of absorber inserts are designed to join them at the crease which does not have absorber material present, so the insert was modeled as two panels centered on each face of the fuel assembly. The inserts were modeled to be the same length as the fuel assembly. Finally, the gadolinium concentration is varied from 0 to 9 wt.% natural gadolinium. The range of concentrations was included because the limitations on the gadolinium loading, absorber initial thickness, and the final in-repository creditable thickness are unknown. If thicknesses larger than 1 mm or gadolinium loadings higher than 2 wt.% can be justified, then it would be possible to estimate the reactivity suppression effect by multiplying the loading by the thickness and then comparing the result to the results of these calculations. It is noted that the clearance between the cell wall (including the neutron absorbers installed in the canister an manufacturing) and the envelope of a fuel assembly (Babcock and Wilcox 15 × 15, which has the largest radial dimension) at loading is 5.16 mm for an MPC-32 and 3.76 mm for a TSC-37. Therefore, implementation of such devices could prove difficult, especially when considering irradiation-induced alterations that the fuel may experience, such as assembly bow. A SCALE-generated depiction of the chevron neutron absorber insert is shown in Figure 8.

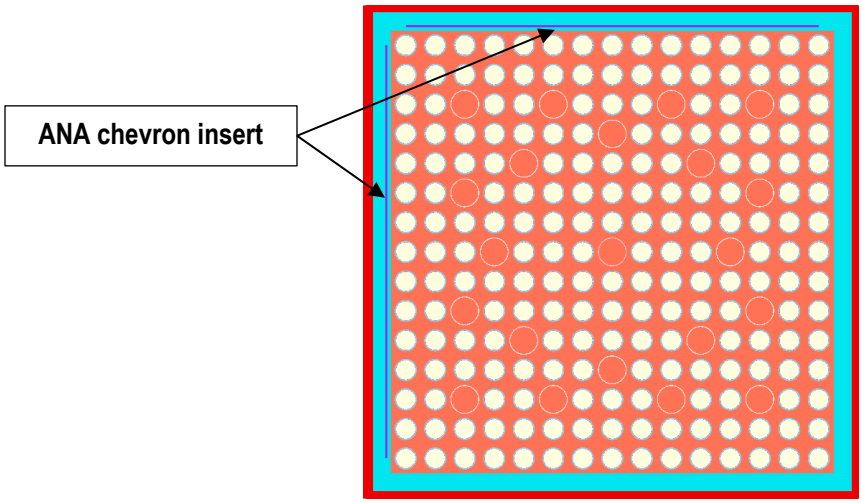


**Figure 8. SCALE-generated depiction of the chevron ANA insert.**

The third and final neutron absorber concept considered in this work is the **ANA BWR replacement fuel channel**. The replacement channels are modeled using the same ANA materials discussed above for the chevron type for PWR fuel. The channels would be fabricated with the same inner dimension as the channels designed by the vendors for use during operation (13.40612 cm) and would be 3 mm thick. The same assumption that these materials would degrade to a thickness of 1 mm in the repository was also applied to the channels. The same gadolinium loading range of 0–9 wt.% was used in the channel calculations to account for potential variation in the original thickness of the channels, the obtainable loading, or the justifiable in repository thickness of the materials. The analysis provided by Hardin and Donovan [5] showed approximately 12 mm of clearance between the basket cell wall of the MPC-89 and the fuel channel, so there should not be a problem to add some width to the channel if necessary above the

channels used during operation. A SCALE-generated depiction of the ANA channel replacement concept is shown in Figure 9.

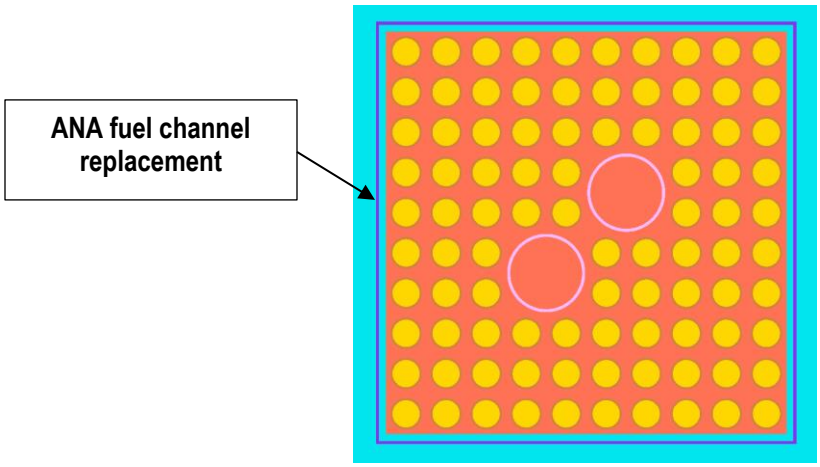


**Figure 9. SCALE-generated depiction of the replacement fuel channels.**

To determine the impact of the absorbers, a few potential loading patterns were considered for each absorber type and canister. Because the fission density plots in Figures 1, 3, and 5 indicate that the majority of the fission would occur in the radially centered section of the DPCs, the number of inserts was increased, starting at the center of the basket. In all cases discussed below, the term *insert* means both the DCRA- and ANA-based chevron absorber. For all of the ANA chevron insert patterns, the absorbers were placed in the upper left corner of the cells unless this would put the absorber on the periphery of the basket. The periphery absorbers were then rotated to face as many fuel assemblies as possible.

For the **TSC-37**, the following loading patterns were considered:

- A 1-insert pattern with a single insert placed in the middle of the basket
- Two patterns with 5 inserts:
    - + pattern with inserts in the center assembly and each of the four face-adjacent assemblies
    - X pattern with inserts in the assemblies diagonally, adjacent to the center assembly
- A 9-insert pattern with inserts in the center assembly and the row adjacent to the center assembly
- A 21-insert pattern with additional inserts in the assemblies that are face-adjacent to the 9-insert pattern assemblies
- A 33-insert pattern with inserts in all locations except for the four damaged fuel locations along the minor axes of the canister on the periphery
- A 37-insert pattern with inserts in all locations.

For the **MPC-32**, the following loading patterns were considered:

- A 2-insert pattern with inserts placed in diagonally adjacent assemblies in the center of the basket
- A 4-insert pattern with inserts in the center four assemblies

- A 12-insert pattern with inserts added to the eight locations face-adjacent to the 4-insert patten locations
- A 16-insert pattern with inserts occupying locations in the inner most two rows of the basket
- A 24-insert pattern with inserts in all locations except the eight corner locations, which can hold damaged fuel (It is noted that there is no damaged fuel in the MPC-32 used for this work)
- A 32-insert pattern with inserts in all locations

For the **MPC-89**, the following ANA channel patterns were considered:

- A 9-channel pattern with ANA channels in the 9 center locations
- A 25-channel pattern with ANA channels in the center two rows adjacent to the center assembly
- A 49-channel pattern with ANA channels in the center three rows adjacent to the center assembly
- A 77-channel pattern with ANA channels in all but the 12 outer locations
- An 89-channel pattern with ANA channels in all locations

The insert and channel-loading patterns are shown in Figure 10 for the TSC-37 canister, Figure 11 for the MPC-32 canister, and Figure 12 for the MPC-89 canister. Locations containing an insert or replacement fuel channel are indicated with an *X*.

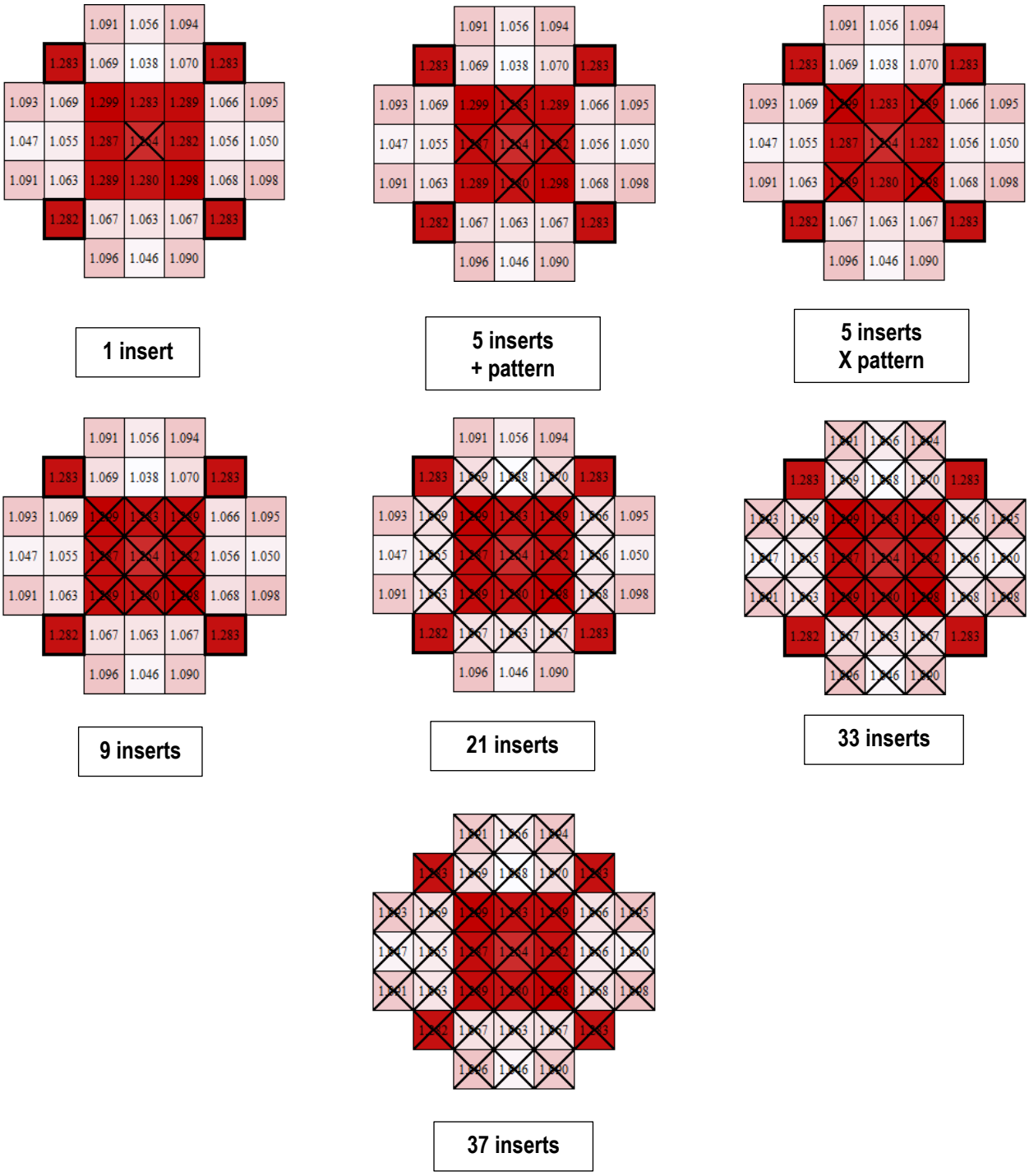


**Figure 10. TSC-37 DCRA and chevron insert loading patterns.**

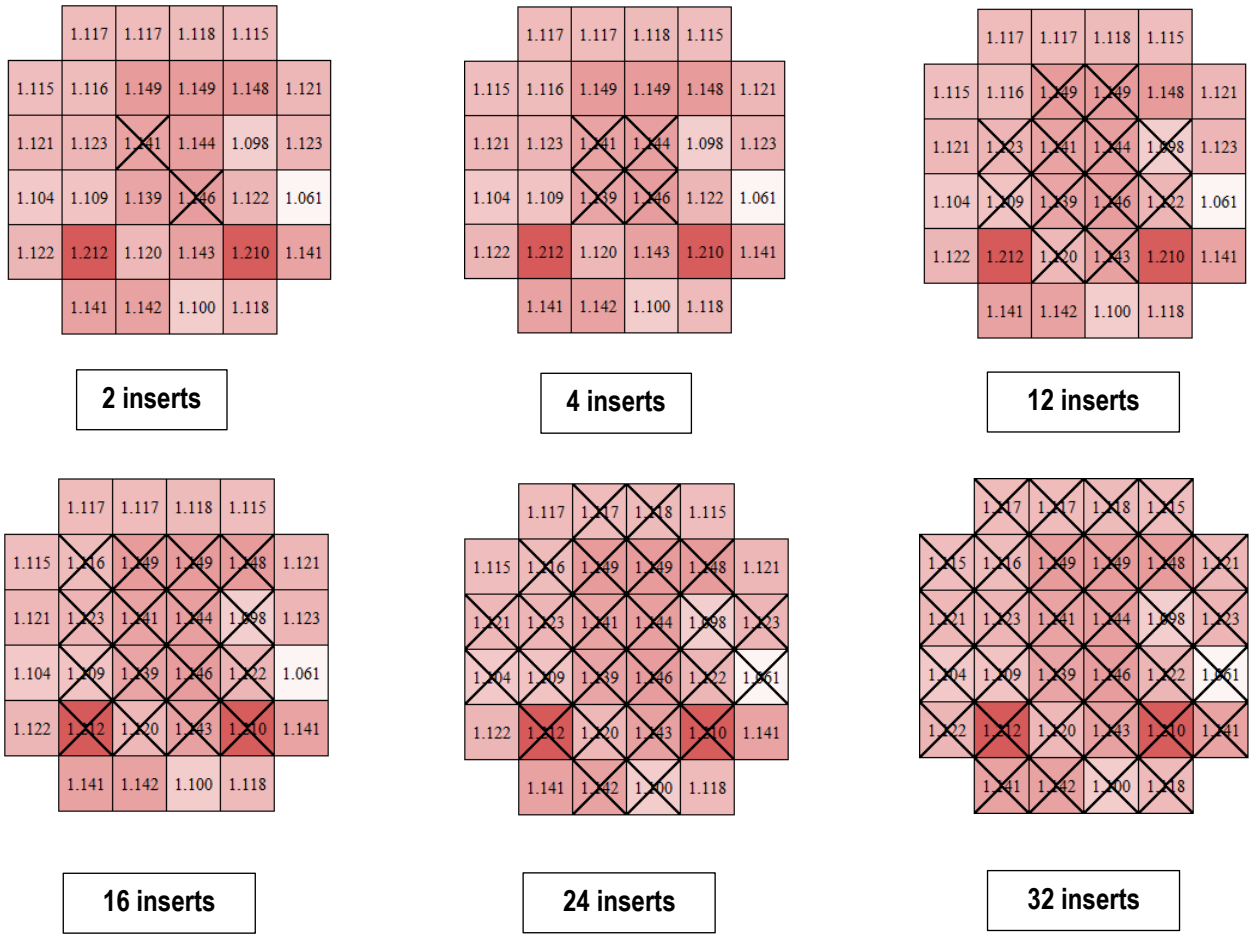


**Figure 11. MPC-32 DCRA and chevron insert loading patterns.**

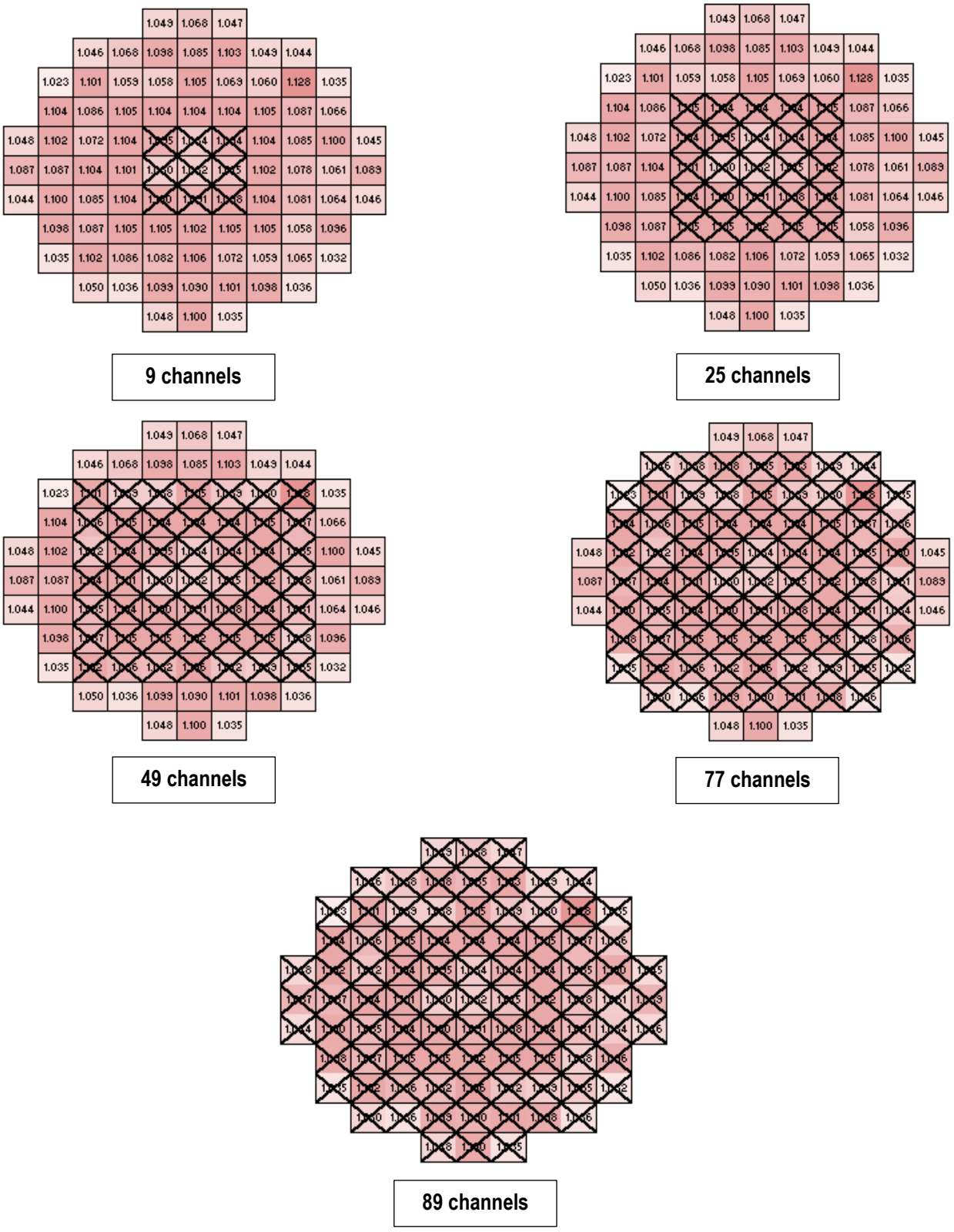


**Figure 12. MPC-89 ANA channel loading patterns.**

# 3. RESULTS AND DISCUSSION

The results of the basket modification calculations discussed in this section are organized by absorber concept. Section 3.1 discusses the DCRA results, Section 3.2 discusses the ANA chevron insert results, and Section 3.3 discusses the ANA channel replacement results. To compare the results, the scale of $k_{eff}$ on the y-axis ranges from 0.70 to 1.20 for all plots in this section. A hypothetical subcritical limit of 0.98 is used here without justification due to the exploratory nature of this work.

## 3.1 DCRA Results

The DCRA concept was examined by running a series of calculations for the TSC-37 NA and DB cases and the MPC-32 NA case using the insert loading patterns shown in Figure 10 for the TSC-37 cases and Figure 11 for the MPC-32 case. The results of the DCRA calculations are shown as a function of $B_4C$ theoretical density for each hypothetical insert loading pattern in Figure 13 for the TSC-37 NA case, Figure 14 for the TSC-37 DB case, and Figure 15 for the MPC-32 NA case.

Based on the results of the TSC-37 NA DCRA calculations presented in Figure 13, it appears that it would take at least five DCRAs, and probably more, with at least 25% of the $B_4C$ theoretical density, to offset the loss of neutron absorbers in the basket (baseline $k_{eff}$ of 1.08619). Both the 5X and 5+patterns performed similarly, and they provide enough hold-down to drop the $k_{eff}$ into the vicinity of the hypothetical limit, with the + pattern offering approximately 0.01 $\Delta k_{eff}$ greater hold-down than the X pattern. Even the 5+ pattern still barely met the hypothetical subcritical limit of 0.98, so it is likely that a higher number of DCRAs would be required to demonstrate subcriticality for this case. The 9-insert pattern dropped the $k_{eff}$ of the NA case system $k_{eff}$ comfortably below the hypothetical limit to a value of ~0.92 for $B_4C$ densities greater than 25% of theoretical density. Additional DCRAs would provide additional margin, although this appears to be relatively saturated between 21- and 31-absorber cases. This saturation effect was likely induced by the flux being forced into the damaged fuel locations, resulting in the stabilization of $k_{eff}$ until those locations were poisoned, as in the 35-insert case. It also appears that the $k_{eff}$ was strongly sensitive to the $B_4C$ density below 25% of theoretical density for all patterns, but it became almost completely insensitive to the $B_4C$ at higher densities in all cases except the 35-insert case. It is also notable that the case used here is among the most reactive examined to date, so it may be more justifiable to use the 5 DCRA patterns for less reactive canisters.

Based on the results of the TSC-37 DB DCRA calculations in presented Figure 14, it appears that it would take at least 21 DCRAs to overcome the loss of neutron absorbers and basket material (baseline $k_{eff}$ of 1.17033). As in the TSC-37 NA case, there was little difference between the 21- and 31-DCRA cases. However, there was less difference between the 31- and 35-DCRA results for the DB case than there was for the NA case. The reduction in the difference between 31- and 35-DCRA results for the DB case may have been caused by the large amount of water introduced into the structural sections of the damaged fuel locations, which may have resulted in the neutronic decoupling of the damaged fuel locations from the remainder of the problem. The same trend in $k_{eff}$ as a function of $B_4C$ density that was observed in the NA case was also present in the DB case.

The results for the MPC-32 NA DCRA calculations in Figure 15 show that it would require at least four and potentially more DCRAs to meet they hypothetical subcritical limit (baseline $k_{eff}$ of 1.02151). The 4-DCRA pattern produced a $k_{eff}$ of ~0.98, depending on the amount of $B_4C$ that can be justified. It would likely be necessary to increase the number of DCRAs for licensing considerations because the 4-DCRA pattern is close to the limit. The 12-DCRA pattern produces results with a comfortable margin to the hypothetical limit, with a $k_{eff}$ of ~0.92. The trend with $B_4C$ is similar to that observed in earlier cases, with strong sensitivity below 10% of theoretical density, and almost complete insensitivity above 25% of theoretical density. There was a relatively smooth increase in the amount of margin for the MPC-32 NA case as the number of inserts was increased. It is also noted that this was the most reactive MPC-32 seen to date, so it is possible that the 4-DCRA pattern would be sufficient for less reactive canisters.

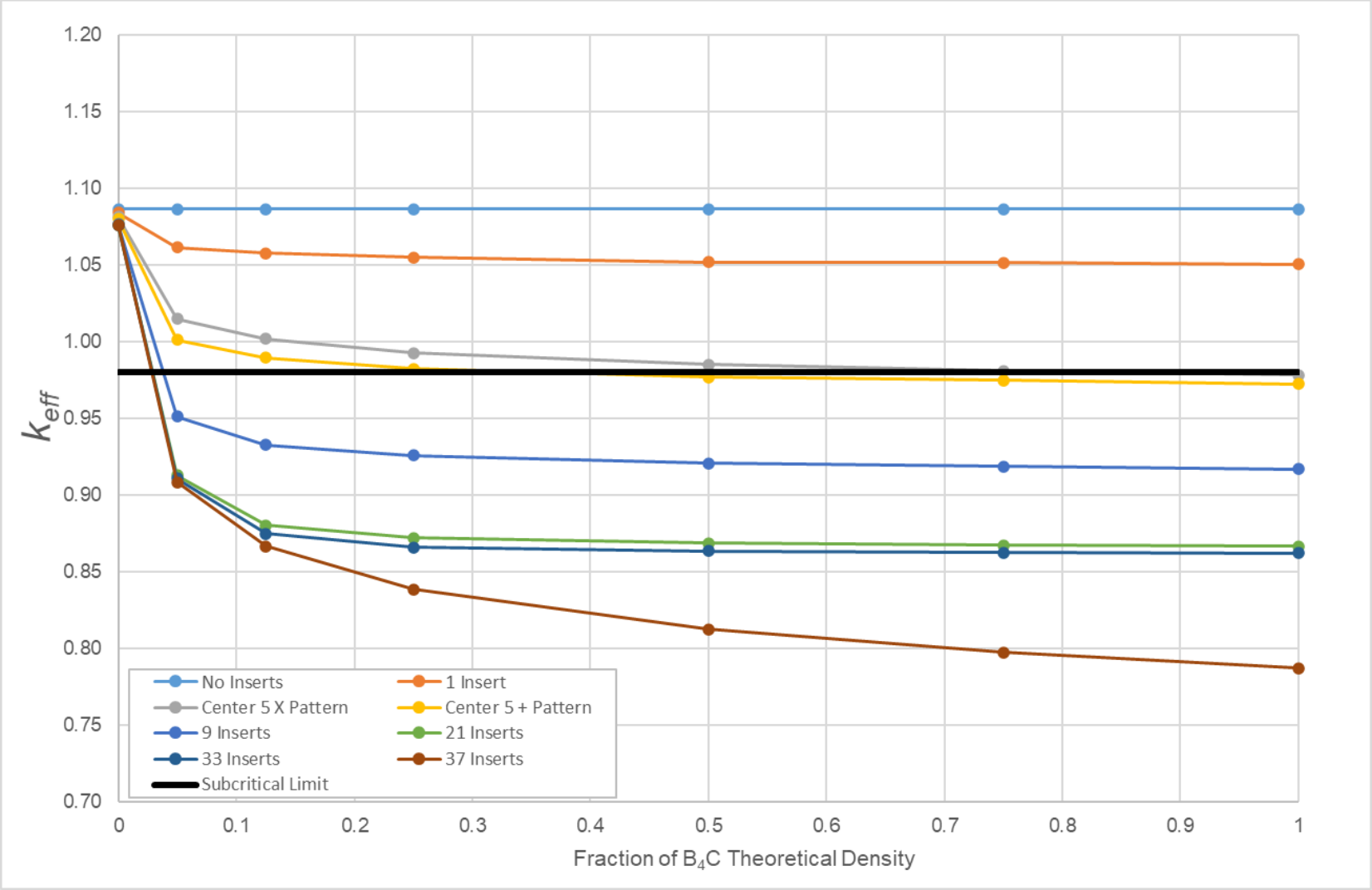


**Figure 13. TSC-37 NA model $k_{eff}$ results as a function of the DCRA pattern and the $B_4C$ fraction of theoretical density.**

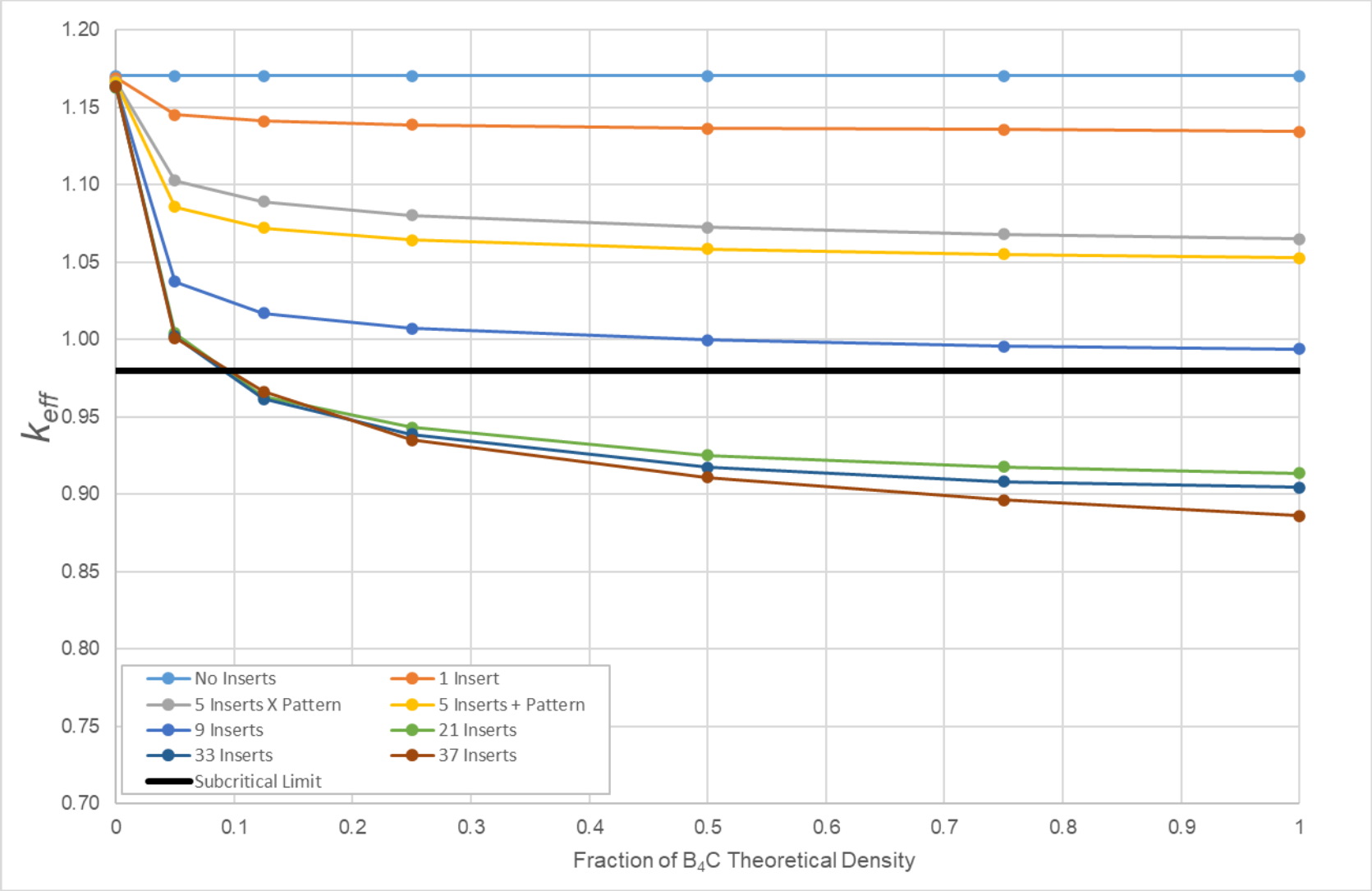


**Figure 14. TSC-37 DB model $k_{eff}$ results as a function of the DCRA pattern and the $B_4C$ fraction of theoretical density.**

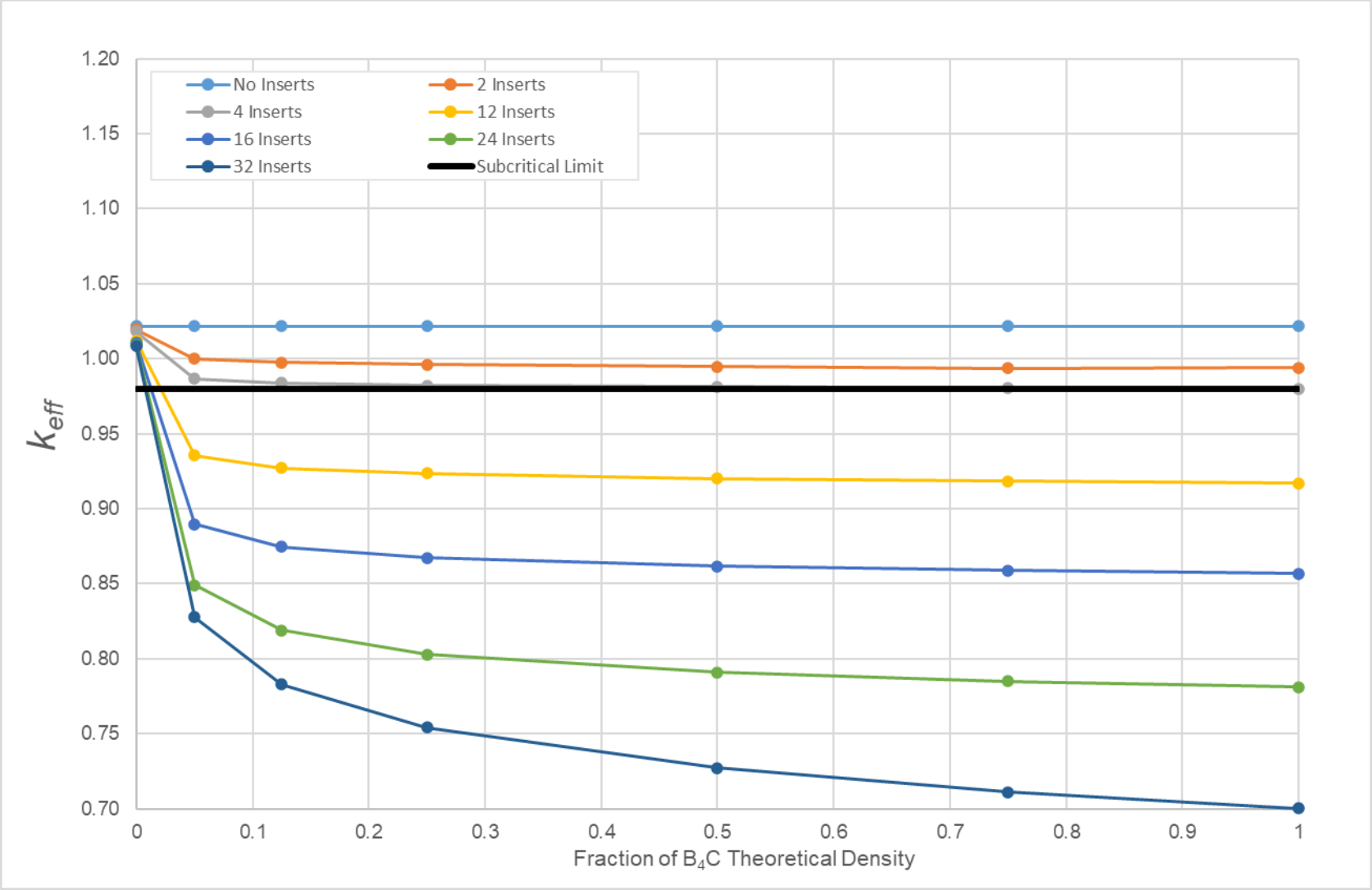


**Figure 15. MPC-32 NA model $k_{eff}$ results as a function of the DCRA pattern and the $B_4C$ fraction of theoretical density.**

## 3.2 ANA Chevron Insert Results

The ANA chevron insert concept was examined by running a series of calculations for the TSC-37 NA and DB cases and the MPC-32 NA case using the insert loading patterns shown in Figure 10 for the TSC-37 cases and Figure 11 for the MPC-32 case. The results of the ANA chevron insert calculations are shown as a function of Gd loading for each hypothetical insert loading pattern in Figure 16 for the TSC-37 NA case, Figure 17 for the TSC-37 DB case, and Figure 18 for the MPC-32 NA case.

The results of the TSC-37 chevron insert calculations for the NA case in Figure 16 and the DB case in Figure 17 indicate that the concept may not be feasible for very high reactivity canister loadings. The calculations show that, regardless of the number of inserts and Gd loading used, it does not appear to be possible to bring the canister $k_{eff}$ below 0.98. It is interesting that both the NA and DB results led to a similar final $k_{eff}$, despite having ~0.10 $\Delta k_{eff}$ baseline $k_{eff}$ values. This is likely due to the addition of water to the basket regions in the DB case when the basket structure was replaced with water. The increase in the amount of water present in the basket likely resulted in more effective absorption by the Gd. It is noted that this is a very high reactivity canister loaded with a number of high reactivity assemblies in the middle, so this represents a very high reactivity basket loading.

The results for the MPC-32 NA chevron insert calculations in Figure 18 show that it may be possible to use the technology to offset absorber loss in canisters that moderately exceed the 0.98 limit. For the MPC-32 case considered here, it appears that at least 12 chevron inserts would be needed to demonstrate subcriticality, although additional margin would be added with additional inserts. It is also apparent that the reactivity effect of Gd effectively saturates for a 1 mm absorber plate at 2 wt.% Gd loading. The saturation effect indicates that it would not be advantageous to justify additional Gd loading or absorber plate thickness.

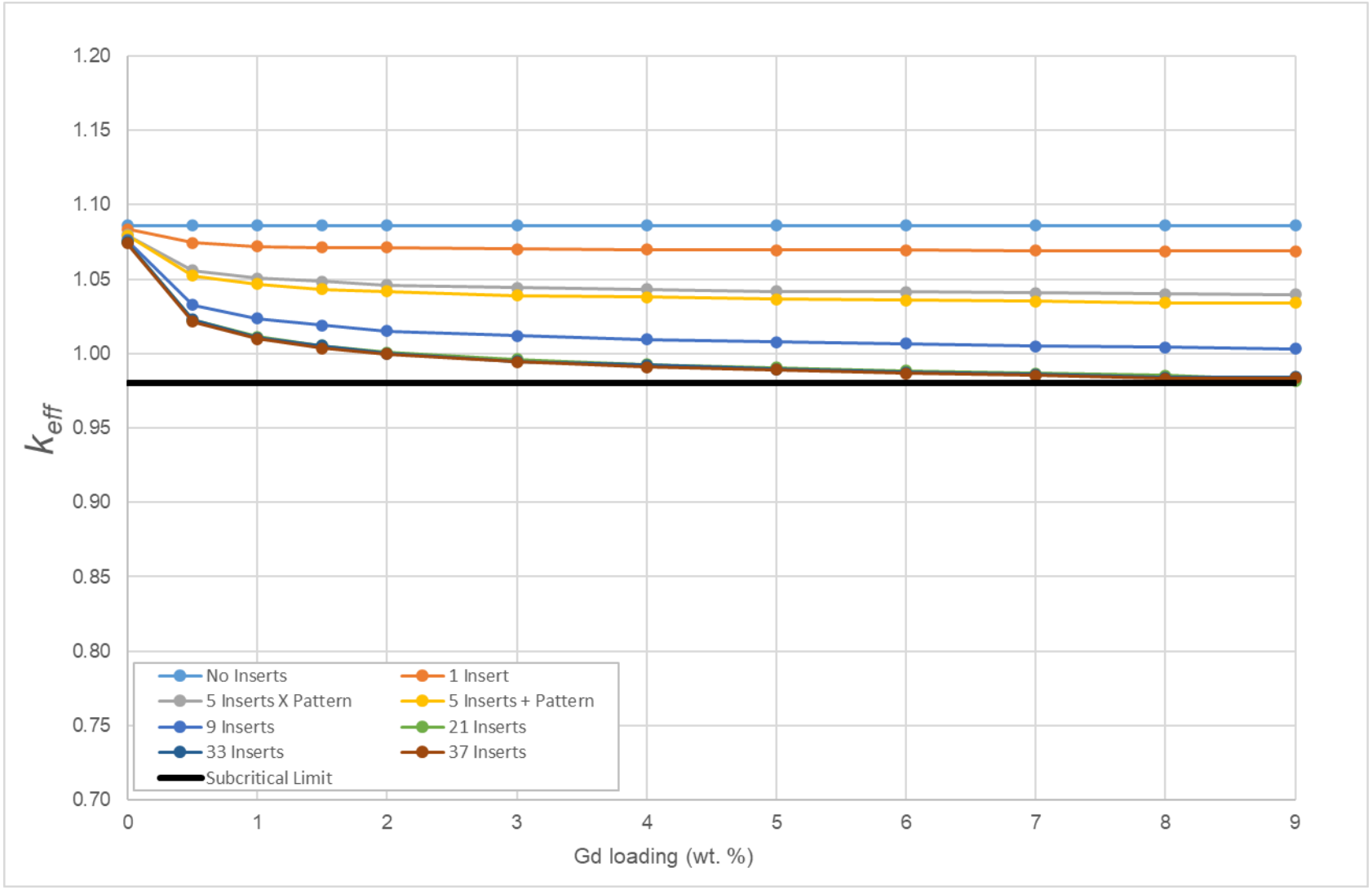


**Figure 16. TSC-37 NA model $k_{eff}$ results as a function of the ANA chevron insert pattern and the Gd loading.**

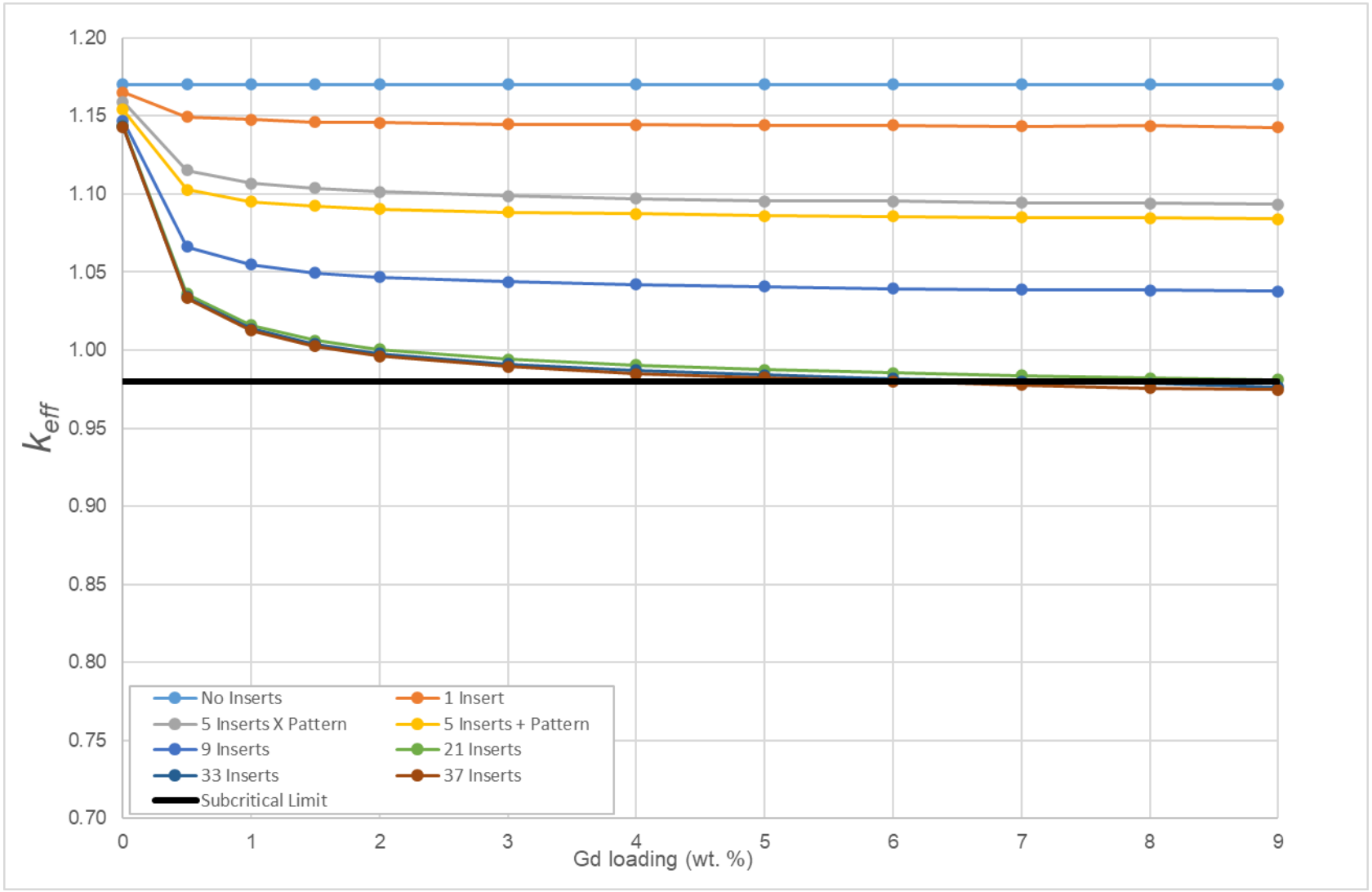


**Figure 17. TSC-37 DB model $k_{eff}$ results as a function of the ANA chevron insert pattern and the Gd loading.**

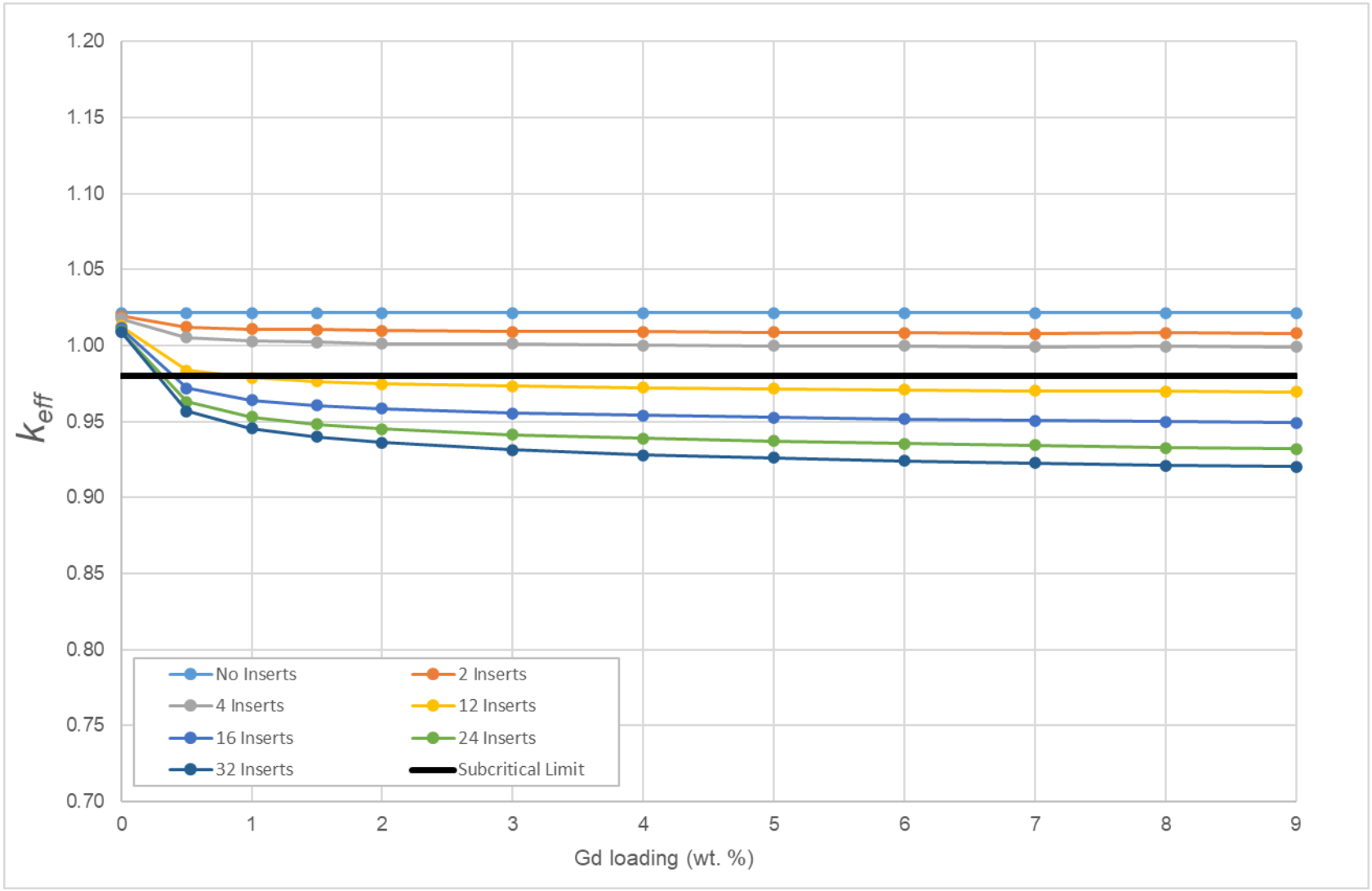


**Figure 18. MPC-32 NA model $k_{eff}$ results as a function of the ANA chevron insert pattern and the Gd loading.**

## 3.3 ANA Channel Replacement Results

The ANA BWR fuel channel replacement concept was examined by running a series of calculations for the MPC-89 using the ANA channel loading patterns shown in Figure 12. The results of the ANA chevron insert calculations are shown as a function of Gd loading for each hypothetical insert loading pattern in Figure 19 for the MPC-89 DB case.

The results of the ANA fuel channel replacement calculations in Figure 19 indicate that 49 channels should be sufficient to offset the reactivity associated with the loss of the neutron absorber basket for the MPC-89. Figure 19 also indicates that there was a strong increase in the amount of reactivity suppression over the baseline calculation (1.18622), with each additional row of channels resulting in several precent $\Delta k_{eff}$. It is also observable that the reactivity suppression effect of increased Gd loadings increased up to 2 wt.%, but it saturated at that point for the relevant loading schemes. There was some sensitivity beyond 2 wt.% for the 77-and 89-channel cases, but those cases are so deeply subcritical that it does not matter.

It is also notable that this is the first set of 89-assembly canisters considered. While the canister used to examine the impact of ANA channel replacement absorbers was the highest $k_{eff}$ among analyzed canisters many of the other canisters had similar reactivities. Therefore, it reasonable to expect that many of the high capacity BWR canisters may also require this type of technology. It also notable that the use of the Metamic-HT material as a structural material causes the use of the DB assumption, resulting in the high canister reactivity. Furthermore, the Holtec 37-assembly PWR canister also uses Metamic-HT as the basket material.

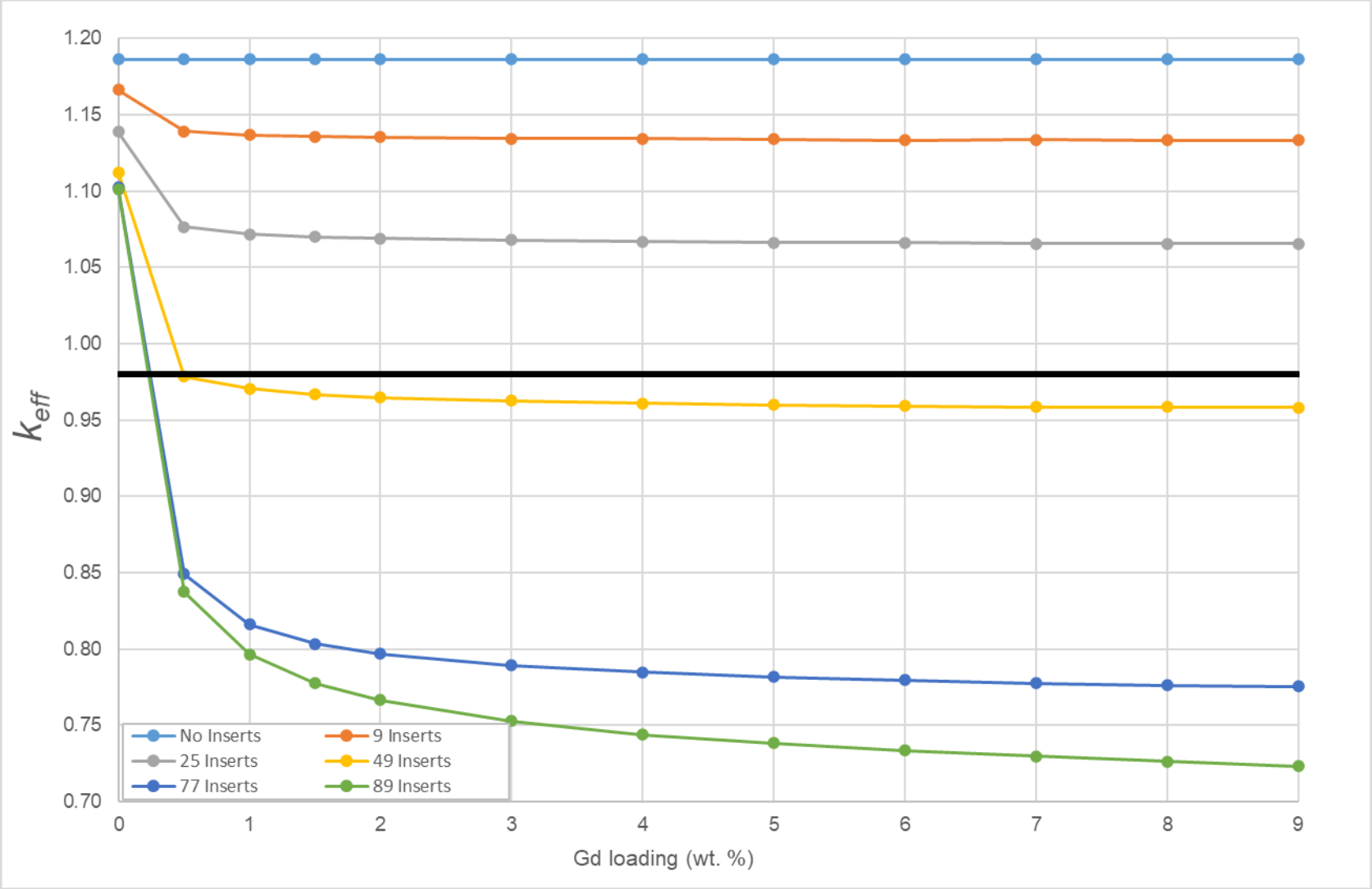


**Figure 19. MPC-89 DB model $k_{eff}$ results as a function of the ANA fuel channel replacement pattern and the Gd loading.**

# 4. CONCLUSIONS AND FUTURE WORK

This report uses three of the most reactive canisters that have been analyzed to date using UNF-ST&DARDS to examine the performance of three potential reactivity suppression technologies under disposal conditions. The canisters used were limiting loadings for the TSC-37 and MPC-32 PWR DPCs and the MPC-89 BWR DPC. The reactivity suppression technologies considered were the $B_4C$-filled DCRA and the ANA-based chevron insert for the PWR canisters and the ANA-based fuel channel replacement absorber for the MPC-89. For each combination of absorber concept and DPC, various insert patterns and absorber material concentrations were considered.

The results of the calculations supporting the DCRA concept are discussed in Section 3.1. The results of TSC-37 calculations for the DCRA concept show that it may be possible to overcome the reactivity increase associated with the NA cases with between 5 and 9 DCRAs, but the DB condition would require a minimum of 21 DCRAs. The results of the MPC-32 DCRA calculations show that it would require between 4 and 12 DCRAs to offset the reactivity increase associated with the NA case. In all cases, a $B_4C$ concentration of 25% of the theoretical density was sufficient to achieve maximum absorber effectiveness, and densities above that value did not improve performance significantly in cases that were not already deeply subcritical.

The results of the calculations supporting the ANA chevron absorber insert discussed in Section 3.2 do not show the ability to offset the reactivity insertion of either NA or DB conditions for the TSC-37 calculations. The results from the MPC-32 calculations show that subcriticality could be demonstrated using at least 12 chevron inserts. It is also noted that there is a loss of sensitivity of $k_{eff}$ to increased Gd loading beyond 2 wt.%. It is unlikely that increased Gd loading or in-repository absorber thickness would improve the results.

The results of the calculations supporting the ANA fuel channel replacement absorber are discussed in Section 3.3. The results of the ANA channel replacement insert show that it is possible to offset the loss of neutron absorber and basket structure with 49 or more channels. As with the chevron inserts composed of ANA, there was an apparent decrease in sensitivity to increased Gd loading beyond 2 wt.%, indicating that justifying additional Gd concentration or thickness of the absorber material would not improve the results beyond that point.

It may be advantageous to explore a wider variety of canisters, canisters loading, and absorber patterns in future work. Doing this would allow for better understanding of the total number of each type of device that would be needed in order to meet fleetwide disposal needs. Additionally, it may be of benefit to examine combine basket modification strategies with upcoming work to optimize the assembly loadings for disposal criticality.

# 5. REFERENCES

1. *Feasibility of Direct Disposal of Dual-Purpose Canisters: Options for Assuring Criticality Control*, EPRI Report 1016629, Electric Power Research Institute, Palo Alto, Calif., 2008.
2. *The Potential of Using Commercial Dual Purpose Canisters for Direct Disposal*, TDR-CRW-SE-000030 Rev 00, US Department of Energy, Office of Civilian Radioactive Waste Management, November 2003.
3. *Handbook of Neutron Absorber Materials for Spent Nuclear Fuel Transportation and Storage Applications*, Electric Power Research Institute, Palo Alto, Calif., 2009.
4. J. B. Clarity et al., *Dual Purpose Canister Reactivity and Groundwater Absorption Analyses, Revision 6*, ORNL/SPR-2020/1724, September 2020.
5. E. H. Hardin and K. P. Donovan, *Options for Future Fuel/Basket Modifications for DPC Disposition*, SAND2020-6236R, Sandia National Laboratories, Albuquerque, NM, June 2020.
6. Rolled Alloys Alloy C22 Data Sheet, https://www.rolledalloys.ca/shared-content/technical-resources/datasheets/C22_DS_US_EN.pdf